*Int. J. Solids Structures* Vol. 27, No. 13, pp. 1721–1738, 1991
Printed in Great Britain.

0020-7683/91 $3.00 + .00


# ALTERNATE BEM FORMULATIONS FOR 2- AND 3-D ANISOTROPIC THERMOELASTICITY

A. DEB and D. P. HENRY, JR
Department of Civil Engineering, School of Engineering and Applied Science,
State University of New York at Buffalo, 240 Ketter Hall, Buffalo, NY 14260, U.S.A.

and

R. B. WILSON
Structures Technology Division, Pratt and Whitney, Hartford, CT 06108, U.S.A.

(*Received* 17 *April* 1990; *in revised form* 9 *July* 1990)

**Abstract**—Direct boundary element formulations are presented for the elastostatic analysis of two- and three-dimensional general anisotropic media subject to known temperature distributions. The thermal effects are incorporated in the analysis through a volume integral or alternatively, using particular integrals. A multi-region boundary element approach is adopted, in which particular integrals are derived assuming a quadratic temperature distribution in each sub-region. A multiple regression scheme is used for the best fit quadratic temperature distribution in each sub-region for temperature data given at discrete points. The multi-region analysis capability of the numerical implementation enhances its capacity to model discontinuous temperature fields as well as piecewise homogeneous media, such as laminated composites. The formulations presented are incorporated in a general purpose system and are illustrated with examples.

## INTRODUCTION

In the most commonly applied uncoupled quasistatic thermoelastic theory, the spatial derivatives of temperature enter the Navier equations of elastostatics with the same effect of an applied body force field. In the context of the conventional direct boundary element formulation, this thermal body force amounts to an additional volume integral (Rizzo and Shippy, 1977). In an alternative approach, the boundary element formulation is stated in terms of complementary solutions of the Navier equations by choosing arbitrary particular integrals, and the above-stated volume integrals warranting volume (domain) discretization can be avoided (Henry and Banerjee, 1988). Until now, the application of the boundary element method (BEM) to problems of thermal stress analysis have been restricted solely to isotropic media. In the present exposition, the BEM is applied to the thermal stress analysis of anisotropic media of the most general form for the first time. Both the volume integration and the particular integral-based approaches are considered. In the latter formulation, the derivation of the particular integrals for the exact modeling of a quadratic temperature distribution is presented. It is of relevance to point out in this context that particular integrals need to be chosen judiciously for competent results. For modeling of an arbitrary temperature distribution given at discrete points, the problem domain may be divided into substructured regions and a quadratic temperature field can be obtained for each sub-region through a multiple regression analysis. The present formulations are incorporated in a general purpose code using second-order isoparametric boundary elements (and volume cells). Numerical examples are presented to illustrate the suitability of these formulations.

## ANISOTROPIC THERMOELASTICITY

The relevant equations (Nowacki, 1986), in the absence of mechanical body forces, for three-dimensional, uncoupled, quasistatic thermoelasticity for an anisotropic medium in terms of net temperature $T(\mathbf{x})$ and displacement field $u_k(\mathbf{x})$ are:

$$\lambda_{ij} T_{,ij} + W = 0 \tag{1}$$

$$c_{ijkl}u_{k,jl} - \beta_{ij}T_{,j} = 0 \quad (i,j,k,l = 1,2,3) \tag{2}$$

where $\lambda_{ij}$ are the thermal conductivities, $W$ is a distributed heat source, $c_{ijkl}$ are the stiffness coefficients and $\beta_{ij} = \alpha_{kl}c_{ijkl}$, $\alpha_{kl}$ being the coefficients of linear thermal expansion. For general anisotropy, there are 21 independent stiffness coefficients $c_{ijkl}$ and six independent thermal coefficients $\alpha_{ij}$. For a problem with well-defined boundary conditions, eqns (1) and (2) bear a cause-and-effect relationship since the solution of eqn (1) provides the necessary body force type input $-\beta_{ij}T_{,j}$ in the Navier eqn (2). Our interest here lies in solving the thermal stress analysis problem represented by (2) by the direct boundary element method, assuming that the task of solving the causal problem of heat conduction (1) has already been carried out. It is noted that for the case of two-dimensional heat conduction with plane strain elasticity, the highest degree of anisotropy permissible corresponds to a material with a plane of symmetry (Lekhnitskii, 1968). For such a material, there are 13 independent elastic constants $c_{ijkl}$ and four independent thermal coefficients $\alpha_{ij}$ (Lekhnitskii, 1968; Padovan, 1986). Thus for the case of plane strain, the last of the eqns (2) is identically satisfied and the thermal stress analysis problem will be reduced to solving two second-order simultaneous differential equations corresponding to $i, j, k, l = 1$ and 2. The case of plane stress is obtained from the plane strain analysis by replacing the material stiffness $c_{ijkl}$ and coefficients of thermal expansion $\alpha_{ij}$ by the corresponding reduced quantities obtained by incorporating the assumptions of generalized plane stress in the Duhamel–Neumann constitutive relations.

## CONVENTIONAL DIRECT BOUNDARY ELEMENT FORMULATION

By treating the quantity $-\beta_{ij}T_{,j}$ in eqn (2) as a body force, the following direct boundary integral equation can be written, using the notation of Banerjee and Butterfield (1981):

$$C_{ij}(\xi)u_i(\xi) = \int_S [G_{ij}(\mathbf{x},\xi)t_i(\mathbf{x}) - F_{ij}(\mathbf{x},\xi)u_i(\mathbf{x})]\,ds(\mathbf{x}) + \int_V B_{ikj}(\mathbf{x},\xi)\beta_{ik}T(\mathbf{x})\,dv(\mathbf{x})$$
$$(i,j,k = 1,2 \text{ in 2D};\ = 1,2,3 \text{ in 3D}) \tag{3}$$

where $G_{ij}(\mathbf{x},\xi)$ are Green's functions or displacement kernels;
$F_{ij}(\mathbf{x},\xi)$ are traction kernels derived using $G_{ij}(\mathbf{x},\xi)$;
$C_{ij}(\xi) = \delta_{ij}$ (Kronecker delta) for interior points and is dependent on surface geometry at $\xi$ for boundary points

$$B_{ikj} = \frac{\partial G_{ij}}{\partial x_k}. \tag{3.1}$$

When $\xi$ is a point on the boundary, the integrals containing the kernels $G_{ij}$ and $B_{ikj}$ are weakly singular and exist in their normal sense, while the integral containing the kernel $F_{ij}$ is strongly singular and exists in the sense of its Cauchy principal value together with a free term that is absorbed on the left-hand side. The Green's functions $G_{ij}$ in eqn (3) are fundamental solutions of the corresponding Navier equations of anisotropic elastostatics for two and three dimensions and are described below.

For the two-dimensional case (Snyder and Cruse, 1975), the fundamental solutions are given by the following closed forms:

$$G_{kj} = 2\,\mathrm{Re}\,[A_{k1}B_{j1}\ln Z_1 + A_{k2}B_{j2}\ln Z_2], \quad (k,j = 1,2) \tag{4}$$

where the quantities on the right of relation (4) are defined below [eqns (4.1) through (4.7)].

The complex constants $A_{kl}$ are given as follows:

$$\begin{Bmatrix} A_{1l} \\ A_{2l} \end{Bmatrix} = \begin{Bmatrix} b_{11}\mu_l^2 + b_{12} - b_{16}\mu_l \\ b_{12}\mu_l + \dfrac{b_{22}}{\mu_l} - b_{26} \end{Bmatrix}, \quad (l = 1, 2). \tag{4.1}$$

The complex quantities $\mu_k$ ($k = 1, 2$), together with the conjugates $\bar{\mu}_k$ ($k = 1, 2$), are the roots of the following fourth-order characteristic equation in terms of reduced stiffness coefficients $b_{ij}$ [eqn (13)]:

$$b_{11}\mu^4 - 2b_{16}\mu^3 + (2b_{12} + b_{66})\mu^2 - 2b_{26}\mu + b_{22} = 0. \tag{4.2}$$

It is assumed above that the $\mu_k$ are the roots of eqn (4.2) with positive imaginary parts.

The complex constants $B_{kl}$ are solutions of the following eqns (4.3)–(4.6):

$$\mu_1 B_{j1} - \bar{\mu}_1 \bar{B}_{j1} + \mu_2 B_{j2} - \bar{\mu}_2 \bar{B}_{j2} = \frac{\delta_{j1}}{2\pi \mathrm{i}}, \quad \mathrm{i} = \sqrt{-1} \tag{4.3}$$

$$B_{j1} - \bar{B}_{j1} + B_{j2} - \bar{B}_{j2} = -\frac{\delta_{j2}}{2\pi \mathrm{i}}, \quad \mathrm{i} = \sqrt{-1} \tag{4.4}$$

$$A_{11} B_{j1} - \bar{A}_{11} \bar{B}_{j1} + A_{12} B_{j2} - \bar{A}_{12} \bar{B}_{j2} = 0 \tag{4.5}$$

$$A_{21} B_{j1} - \bar{A}_{21} \bar{B}_{j1} + A_{22} B_{j2} - \bar{A}_{22} \bar{B}_{j2} = 0 \tag{4.6}$$

[$j = 1, 2$ in equations (4.3) (4.6)].

The complex variables $Z_k$ ($k = 1, 2$) are defined as

$$Z_k = (x_1 - \xi_1) + \mu_k (x_2 - \xi_2). \tag{4.7}$$

The traction kernel $F_{ij}(\mathbf{x}, \xi)$ in eqn (3) is obtained by suitable differentiations of $G_{ij}(\mathbf{x}, \xi)$ and appropriate applications of the constitutive relations and the Cauchy equilibrium equations on the boundary.

In previous applications of the boundary element method for general anisotropy in three dimensions, Vogel and Rizzo (1973) and Wilson and Cruse (1978) used Green's functions in the following form (Synge, 1957):

$$G_{ij}(\mathbf{x}, \xi) = \frac{1}{8\pi^2 |\mathbf{x} - \xi|} \oint_{|t|=1} K_{ij}^{-1}(t)\, \mathrm{d}s, \quad (i, j = 1, 2, 3) \tag{5}$$

where the line integral is taken on the unit circle in the plane normal to the vector $(\mathbf{x} - \xi)$ and passing through $\mathbf{x}$, and the function

$$K_{ij}^{-1}(t) = [c_{ijkm} t_k t_m]^{-1}. \tag{5.1}$$

Since it is not possible to evaluate the line integral of eqn (5) in closed form for the general case, numerical integration was employed. The boundary element procedure based on the above numerically-computed Green's functions proved to be extremely time consuming despite improvements in which interpolation schemes are used to avoid actually using relationship (5) at every Gauss point (Wilson and Cruse, 1978). A more efficient approach is adopted in the present work in which the Green's functions are calculated at the grid points and bivariate cubic spline functions are then fitted through these points for the purpose of interpolation. The Green functions adopted in the present work can be

expressed in terms of spherical coordinates as:

$$G_{ij}(r,\theta,\phi) = -\frac{1}{4\pi r}\sum_{\nu=1}^{6}\text{Sign}\,(\text{Re}(\nu))\eta_i(\nu)\eta_j(\nu), \quad (i,j=1,2,3) \tag{6}$$

where, in the real variable formulation, the $\nu$ and $\eta(\nu)$ are the eigenvalues and eigenvectors of a $6\times 6$ real matrix (Malen, 1971). The eigenvalues and eigenvectors occur as complex conjugates. The $\phi$ derivative of $G_{ij}$ can be expressed as

$$G_{ij,\phi} = -\frac{1}{4\pi r}\sum_{\nu=1}^{6}\text{Sign}\,(\text{Re}(\nu))\left[\frac{\partial\eta_i(\nu)}{\partial\phi}\eta_j(\nu)+\eta_i(\nu)\frac{\partial\eta_j(\nu)}{\partial\phi}\right], \quad (i,j=1,2,3) \tag{7}$$

with a similar expression for $G_{ij,\theta}$. These derivatives are required for the computation of the traction kernels $F_{ij}$. For the purpose of calculating interior stresses and strains, the necessary second derivatives have also been developed.

The boundary element implementation of eqn (3) entails not only boundary discretization, but also discretization of the domain. Quadratic isoparametric elements are chosen to this end for both two- and three-dimensional analyses. The solution of the boundary value problem is carried out in a standard way (Cruse, 1973, 1974; Lachat and Watson, 1976; Watson, 1979; Banerjee and Butterfield, 1981) with the volume integral in eqn (3) making an additional contribution to the right-hand side vector in the system equations.

## INTERIOR STRESS CALCULATION BY VOLUME INTEGRATION

The integral equation for strain at an interior point is found analytically by substituting eqn (3) (with $C_{ij}=\delta_{ij}$) into the strain–displacement relations, where differentiation is with respect to the field point $\xi$:

$$\varepsilon_{ij}(\xi) = \int_S [G^{\varepsilon}_{kij}(\mathbf{x},\xi)t_k(\mathbf{x}) - F^{\varepsilon}_{kij}(\mathbf{x},\xi)u_k(\mathbf{x})]\,ds(\mathbf{x}) + \int_V B^{\varepsilon}_{klij}(\mathbf{x},\xi)\beta_{kl}T(\mathbf{x})\,dv(\mathbf{x}) + J^{\varepsilon}_{klij}\beta_{kl}T(\xi). \tag{8}$$

By introducing the above equation into the Duhamel–Neumann constitutive relation by linear thermal expansion (viz. $\sigma_{ij} = c_{ijkl}\varepsilon_{kl} - \beta_{ij}T$), the stress integral equation is derived:

$$\sigma_{ij}(\xi) = \int_S [G^{\sigma}_{kij}(\mathbf{x},\xi)t_k(\mathbf{x}) - F^{\sigma}_{kij}(\mathbf{x},\xi)u_k(\mathbf{x})]\,ds(\mathbf{x}) + \int_V B^{\sigma}_{klij}(\mathbf{x},\xi)\beta_{kl}T(\mathbf{x})\,dv(\mathbf{x}) + J^{\sigma}_{klij}\beta_{kl}T(\xi). \tag{9}$$

The volume integrals in eqns (8) and (9) are strongly singular and are to be interpreted in the Cauchy principal value sense with free terms containing $J^{\varepsilon}_{klij}$ and $J^{\sigma}_{klij}$. An accurate numerical integration of these volume integrals over a singular point is difficult (Banerjee and Raveendra, 1986). Nevertheless, for an interior point coinciding with a cell node, the singular coefficients may be evaluated indirectly by the initial stress expansion technique (Banerjee *et al.*, 1989). The operation is analogous to the rigid body technique (Rizzo and Shippy, 1968; Watson, 1979; Banerjee and Butterfield, 1981) which employs a rigid body solution for the indirect calculation of the singular coefficient of the $F_{ij}$ kernel of the boundary displacement integral equation. In the present case, an anisotropic body is subjected to a uniform initial stress and is free to expand, resulting in a stress-free state of stress through the body. The resulting displacement is linear and is determined analytically. After the coefficients of the $B^{\sigma}_{klij}$ kernel related to the non-singular nodes are determined by numerical integration, the coefficients corresponding to the singular node are found by imposing the solution for a uniform initial stress state on the boundary integral stress equation.

To clarify this point, let eqn (9) be written in matrix form for an interior point which is a cell node as follows:

$$\bar{\sigma} = \mathbf{G}^{\sigma}\bar{t} - \mathbf{F}^{\sigma}\bar{u} + \mathbf{B}^{\sigma}\bar{\sigma}^{0} \tag{10}$$

where it has been assumed that $\bar{\sigma}^0$ is the nodal vector corresponding to the initial stress $\sigma_{ij}^0$ defined as

$$\sigma_{ij}^{0}(\mathbf{x}) = \beta_{ij}T(\mathbf{x}) \tag{10.1}$$

and $J_{kli}^{\sigma}$ associated with the free term has been absorbed in $\mathbf{B}^{\sigma}$.

In order to compute the singular coefficients of $\mathbf{B}^{\sigma}$ in eqn (10) corresponding to singular nodes, six independent admissible initial stress states (or three in two dimensions) are considered for the evaluation of six (or three) "singular node" coefficients in each equation. These initial stress states do not give rise to any stresses in the elastic continuum and in effect correspond to states of free thermal expansion. Thus, for the chosen initial stress states, eqn (10) becomes

$$\mathbf{B}^{\sigma}\bar{\sigma}^{0} = \mathbf{F}^{\sigma}\bar{u}. \tag{11}$$

With the substitution of each independent initial stress state and corresponding displacements, one singular coefficient per equation in matrix $\mathbf{B}^{\sigma}$ can be accurately evaluated. The initial stress states and the resulting displacement fields are given in Tables 1 and 2. The compliance coefficients $b_{ij}$ appearing in the displacement fields are actual material properties for 3D and are appropriate reduced or effective properties (Lekhnitskii, 1968) for 2D (plane stress/strain condition). Implicit in the foregoing statement are the following forms of the Duhamel Neumann constitutive relation relating engineering strains to stresses:

for 3D,

$$\begin{Bmatrix} \varepsilon_{11} \\ \varepsilon_{22} \\ \varepsilon_{33} \\ \gamma_{23} \\ \gamma_{13} \\ \gamma_{12} \end{Bmatrix} = \begin{bmatrix} b_{11} & b_{12} & b_{13} & b_{14} & b_{15} & b_{16} \\ & b_{22} & b_{23} & b_{24} & b_{25} & b_{26} \\ & & b_{33} & b_{34} & b_{35} & b_{36} \\ & \text{symmetric} & & b_{44} & b_{45} & b_{46} \\ & & & & b_{55} & b_{56} \\ & & & & & b_{66} \end{bmatrix} \begin{Bmatrix} \sigma_{11} \\ \sigma_{22} \\ \sigma_{33} \\ \sigma_{23} \\ \sigma_{13} \\ \sigma_{12} \end{Bmatrix} + \begin{Bmatrix} \alpha_{11} \\ \alpha_{22} \\ \alpha_{33} \\ \alpha_{23} \\ \alpha_{13} \\ \alpha_{12} \end{Bmatrix} T \tag{12}$$

for 2D,

$$\begin{Bmatrix} \varepsilon_{11} \\ \varepsilon_{22} \\ \gamma_{12} \end{Bmatrix} = \begin{bmatrix} b_{11} & b_{12} & b_{16} \\ & b_{22} & b_{26} \\ \text{symmetric} & & b_{66} \end{bmatrix} \begin{Bmatrix} \sigma_{11} \\ \sigma_{22} \\ \sigma_{12} \end{Bmatrix} + \begin{Bmatrix} \alpha_{11} \\ \alpha_{22} \\ \alpha_{12} \end{Bmatrix} T. \tag{13}$$

Table 1. Stress states for initial stress expansion technique in two-dimensional plane strain (plane stress) analysis

| Stress state | Element to be determined corresponds to | Nodal values of assumed stress state | | | | |
|---|---|---|---|---|---|---|
| | | $\sigma_{11}^0$ | $\sigma_{22}^0$ | $\sigma_{12}^0$ | $u_1$ | $u_2$ |
| 1 | $\sigma_{11}^0$ | 1 | 0 | 0 | $b_{11}x_1 + \frac{1}{2}b_{16}x_2$ | $b_{12}x_2 + \frac{1}{2}b_{16}x_1$ |
| 2 | $\sigma_{22}^0$ | 0 | 1 | 0 | $b_{12}x_1 + \frac{1}{2}b_{26}x_2$ | $b_{22}x_2 + \frac{1}{2}b_{26}x_1$ |
| 3 | $\sigma_{12}^0$ | 0 | 0 | 1 | $b_{16}x_1 + \frac{1}{2}b_{66}x_2$ | $b_{26}x_2 + \frac{1}{2}b_{66}x_1$ |

Table 2. Stress state for initial stress expansion technique in three-dimensional analysis

| Stress state | Element to be determined corresponds to | Nodal values of assumed stress state | | | | | | | | |
|---|---|---|---|---|---|---|---|---|---|---|
| | | $\sigma_{11}^0$ | $\sigma_{22}^0$ | $\sigma_{33}^0$ | $\sigma_{23}^0$ | $\sigma_{13}^0$ | $\sigma_{12}^0$ | $u_1$ | $u_2$ | $u_3$ |
| 1 | $\sigma_{11}^0$ | 1 | 0 | 0 | 0 | 0 | 0 | $b_{11}x_1+\frac{1}{2}b_{16}x_2+\frac{1}{2}b_{15}x_3$ | $\frac{1}{2}b_{16}x_1+b_{12}x_2+\frac{1}{2}b_{14}x_3$ | $\frac{1}{2}b_{15}x_1+\frac{1}{2}b_{14}x_2+b_{13}x_3$ |
| 2 | $\sigma_{22}^0$ | 0 | 1 | 0 | 0 | 0 | 0 | $b_{12}x_1+\frac{1}{2}b_{26}x_2+\frac{1}{2}b_{25}x_3$ | $\frac{1}{2}b_{26}x_1+b_{22}x_2+\frac{1}{2}b_{24}x_3$ | $\frac{1}{2}b_{25}x_1+\frac{1}{2}b_{24}x_2+b_{23}x_3$ |
| 3 | $\sigma_{33}^0$ | 0 | 0 | 1 | 0 | 0 | 0 | $b_{13}x_1+\frac{1}{2}b_{36}x_2+\frac{1}{2}b_{35}x_3$ | $\frac{1}{2}b_{36}x_1+b_{32}x_2+\frac{1}{2}b_{34}x_3$ | $\frac{1}{2}b_{35}x_1+\frac{1}{2}b_{34}x_2+b_{33}x_3$ |
| 4 | $\sigma_{23}^0$ | 0 | 0 | 0 | 1 | 0 | 0 | $b_{14}x_1+\frac{1}{2}b_{46}x_2+\frac{1}{2}b_{45}x_3$ | $\frac{1}{2}b_{46}x_1+b_{24}x_2+\frac{1}{2}b_{44}x_3$ | $\frac{1}{2}b_{45}x_1+\frac{1}{2}b_{44}x_2+b_{34}x_3$ |
| 5 | $\sigma_{13}^0$ | 0 | 0 | 0 | 0 | 1 | 0 | $b_{15}x_1+\frac{1}{2}b_{56}x_2+\frac{1}{2}b_{55}x_3$ | $\frac{1}{2}b_{56}x_1+b_{25}x_2+\frac{1}{2}b_{45}x_3$ | $\frac{1}{2}b_{55}x_1+\frac{1}{2}b_{45}x_2+b_{35}x_3$ |
| 6 | $\sigma_{12}^0$ | 0 | 0 | 0 | 0 | 0 | 1 | $b_{16}x_1+\frac{1}{2}b_{66}x_2+\frac{1}{2}b_{56}x_3$ | $\frac{1}{2}b_{66}x_1+b_{26}x_2+\frac{1}{2}b_{46}x_3$ | $\frac{1}{2}b_{56}x_1+\frac{1}{2}b_{46}x_2+b_{36}x_3$ |

## DIRECT BOUNDARY ELEMENT FORMULATION USING PARTICULAR INTEGRALS

In order to use the boundary element method for solving problems involving body forces without recourse to time-consuming volume integration, the method of particular integrals for solving inhomogeneous differential equations has been applied (Jaswon and Maiti, 1968; Pape and Banerjee, 1987). In the context of thermal stress analysis of an isotropic medium by the direct boundary element method, a particular integral-based approach was used first by Henry and Banerjee (1988). A similar approach has been followed here for the case of general anisotropy on a plane and in three dimensions. The essence of the approach lies in transforming the linear, inhomogeneous differential equation (2) into a homogeneous form by assuming that the displacement field $u_i$ can be expressed as the sum of a complementary function, $u_i^c$, and an arbitrary particular integral, $u_i^p$. Thus, we have the following relations in sequence:

$$u_i = u_i^c + u_i^p \tag{14}$$

$$c_{ijkl}u_{k,lj} - \beta_{ij}T_{,j} = 0 \tag{15}$$

$$c_{ijkl}u_{k,lj}^c = 0. \tag{16}$$

The boundary integral statement for eqn (16) is similar to eqn (3) without the volume integral. In the discretized form of the boundary integral equations, the complementary functions (i.e. displacements $u_i^c$ and tractions $t_i^c$) are replaced by the corresponding total functions ($u_i$ and $t_i$) minus the particular integrals ($u_i^p$ and $t_i^p$). The linear system of equations prior to the application of the boundary conditions may thus be written using matrix notation as (Pape and Banerjee, 1987):

$$\mathbf{G}\bar{t} - \mathbf{F}\bar{u} = \mathbf{G}\bar{t}^p - \mathbf{F}\bar{u}^p. \tag{17}$$

Nodal values of the particular integral for displacements and tractions are substituted in eqn (17) and the system can then be solved for a set of well-posed boundary conditions. The particular integrals which must satisfy eqn (15) are non-unique. This non-uniqueness of the particular integrals, however, does not imply a loss of uniqueness in the total solution since the complementary function will adjust for different particular integrals yielding a unique total solution for the applied boundary conditions. Nevertheless, certain particular integrals are numerically more stable than others in the boundary element implementation. As a general guideline for polynomial-type body forces, the particular integrals for stresses satisfying equilibrium and compatibility conditions should be complete polynomials of an order higher than the applied body force.

The particular integrals derived in the present work assume a quadratic temperature distribution. For an arbitrary temperature distribution given at discrete points, the best quadratic fit in the least-squares error sense is generated through a multiple regression analysis. Since the applied temperatures are modeled region by region, it is possible to account for temperature discontinuities across an interface of two or more regions. The application of the present particular integral-based approach is thus quite general and the accuracy of the results is governed solely by the degree of approximation in the modeling of the temperature field.

An orderly procedure will now be outlined leading to the particular integrals due to a quadratic temperature distribution in the two-dimensional case. An analogous procedure of derivation may be followed for the three-dimensional analysis.

Let us start with assuming the temperature distribution on the plane to be

$$T(x_1, x_2) = t_0 + t_1x_1 + t_2x_2 + t_{11}x_1^2 + t_{12}x_1x_2 + t_{22}x_2^2 \tag{18}$$

where the coefficients $t_0, t_1, \ldots, t_{22}$ are obtained by a multiple regression analysis from temperature data given at discrete points across a sub-region.

Upon inspection of the governing equations, quadratic polynomials are assumed for the particular integrals for stress. The most suitable forms of particular integrals were found to be:

$$\sigma_{11}^{p} = r_1 x_1 + r_2 x_1^2 + r_3 x_1 x_2 \tag{19.1}$$

$$\sigma_{22}^{p} = r_4 x_2 + r_5 x_1 x_2 + r_6 x_2^2 \tag{19.2}$$

$$\sigma_{12}^{p} = r_7 x_1 + r_8 x_2 + r_9 x_1^2 + r_{10} x_1 x_2 + r_{11} x_2^2 \tag{19.3}$$

where the 11 unknown coefficients need to be determined non-trivially. The particular integrals (19.1)–(19.3) should satisfy the following equations of equilibrium:

$$\sigma_{11,1} + \sigma_{12,2} = 0 \tag{20.1}$$

$$\sigma_{12,1} + \sigma_{22,2} = 0. \tag{20.2}$$

Upon substituting relations (19.1)–(19.3) in eqns (20.1)–(20.2), we get the following six homogeneous relations in the 11 unknown stress coefficients:

$$r_1 + r_8 = 0 \tag{21}$$

$$2r_2 + r_{10} = 0 \tag{22}$$

$$r_3 + 2r_{11} = 0 \tag{23}$$

$$r_7 + r_4 = 0 \tag{24}$$

$$2r_9 + r_5 = 0 \tag{25}$$

$$r_{10} + 2r_6 = 0. \tag{26}$$

To obtain the five additional equations for a solution of $r_i$ ($i = 1$–$11$), the Duhamel–Neumann stress–strain relations (13) will be applied in conjunction with the strain–displacement relations of linear two-dimensional elasticity.

Incorporating the linear strain–displacement relations, the Duhamel–Neumann constitutive relation (13) becomes

$$\varepsilon_{11} = u_{1,1} = b_{11}\sigma_{11} + b_{12}\sigma_{22} + b_{16}\sigma_{12} + \alpha_{11}T \tag{27.1}$$

$$\varepsilon_{12} = u_{2,2} = b_{12}\sigma_{11} + b_{22}\sigma_{22} + b_{26}\sigma_{12} + \alpha_{22}T \tag{27.2}$$

$$\gamma_{12} = u_{1,2} + u_{2,1} = b_{16}\sigma_{11} + b_{26}\sigma_{22} + b_{66}\sigma_{12} + \alpha_{12}T. \tag{27.3}$$

On substituting the stresses (19.1)–(19.3) and the temperature field (18) in eqns (27.1)–(27.3) above, we have

$$u_{1,1}^{p} = p_0^{(1)} + p_1^{(1)} x_1 + p_2^{(1)} x_2 + p_{11}^{(1)} x_1^2 + p_{12}^{(1)} x_1 x_2 + p_{22}^{(1)} x_2^2 \tag{28.1}$$

$$u_{2,2}^{p} = p_0^{(2)} + p_1^{(2)} x_1 + p_2^{(2)} x_2 + p_{11}^{(2)} x_1^2 + p_{12}^{(2)} x_1 x_2 + p_{22}^{(2)} x_2^2 \tag{28.2}$$

$$u_{1,2}^{p} + u_{2,1}^{p} = p_0^{(6)} + p_1^{(6)} x_1 + p_2^{(6)} x_2 + p_{11}^{(6)} x_1^2 + p_{12}^{(6)} x_1 x_2 + p_{22}^{(6)} x_2^2 \tag{28.3}$$

where

$$p_0^{(i)} = \alpha_{ii} t_0 \tag{29.1}$$

$$p_1^{(i)} = b_{i1} r_1 + b_{i6} r_7 + \alpha_{ii} t_1 \tag{29.2}$$

$$p_2^{(i)} = b_{i2} r_4 + b_{i6} r_8 + \alpha_{ii} t_2 \tag{29.3}$$

$$p_{11}^{(i)} = b_{i1}r_2 + b_{i6}r_9 + \alpha_{ii}t_{11} \tag{29.4}$$

$$p_{12}^{(i)} = b_{i1}r_3 + b_{i2}r_5 + b_{i6}r_{10} + \alpha_{ii}t_{12} \tag{29.5}$$

$$p_{22}^{(i)} = b_{i2}r_6 + b_{i6}r_{11} + \alpha_{ii}t_{22}. \tag{29.6}$$

In relations (29.1)–(29.6) above, $i = 1, 2$ and 6, $b_{ij} = b_{ji}$ and $\alpha_{66} = \alpha_{12}$.

Integration of eqn (28.1) with respect to $x_1$ and of eqn (28.2) with respect to $x_2$ yields the following expressions for the displacements:

$$u_1^p = p_0^{(1)}x_1 + \tfrac{1}{2}p_1^{(1)}x_1^2 + p_2^{(1)}x_1x_2 + \tfrac{1}{3}p_{11}^{(1)}x_1^3 + \tfrac{1}{2}p_{12}^{(1)}x_1^2x_2 + p_{22}^{(1)}x_1x_2^2 + I_1(x_2) \tag{30.1}$$

$$u_2^p = p_0^{(2)}x_2 + \tfrac{1}{2}p_2^{(2)}x_2^2 + p_1^{(2)}x_1x_2 + \tfrac{1}{3}p_{22}^{(2)}x_2^3 + \tfrac{1}{2}p_{12}^{(2)}x_1x_2^2 + p_{11}^{(2)}x_1^2x_2 + I_2(x_1) \tag{30.2}$$

where $I_1(x_2)$ and $I_2(x_1)$ are constants of integration.

Substituting expressions given by (30.1) and (30.2) in eqn (28.3) and rearranging, we obtain:

$$(p_2^{(1)} - p_1^{(6)})x_1 + (p_1^{(2)} - p_2^{(6)})x_2 + (\tfrac{1}{2}p_{12}^{(1)} - p_{11}^{(6)})x_1^2 + (2p_{22}^{(1)} + 2p_{11}^{(2)} - p_{12}^{(6)})x_1x_2 + (\tfrac{1}{2}p_{12}^{(2)} - p_{22}^{(6)})x_2^2 + I_{1,2} + I_{2,1} - p_0^{(6)} = 0. \tag{31}$$

For relation (31) to be an identity, we must have:

$$p_2^{(1)} - p_1^{(6)} = 0 \tag{32}$$

$$p_1^{(2)} - p_2^{(6)} = 0 \tag{33}$$

$$\tfrac{1}{2}p_{12}^{(1)} - p_{11}^{(6)} = 0 \tag{34}$$

$$2p_{22}^{(1)} + 2p_{11}^{(2)} - p_{12}^{(6)} = 0 \tag{35}$$

$$\tfrac{1}{2}p_{12}^{(2)} - p_{22}^{(6)} = 0 \tag{36}$$

$$I_{1,2} + I_{2,1} - p_0^{(6)} = 0. \tag{37}$$

Equation (37) above can be satisfied if $I_1$ and $I_2$ are chosen to be the following:

$$I_1 = \tfrac{1}{2}p_0^{(6)}x_2 = \tfrac{1}{2}\alpha_{12}t_0x_2 \tag{38.1}$$

$$I_2 = \tfrac{1}{2}p_0^{(6)}x_1 = \tfrac{1}{2}\alpha_{12}t_0x_1. \tag{38.2}$$

Using relations (29.1)–(29.6) in eqns (32)–(36), we get five additional equations for the unknown stress coefficients $r_i$ ($i = 1$–11). Together with the six equations (21)–(26), we thus have 11 equations for solving 11 quantities $r_i$. It may be noted that the coefficients $r_i$, being dependent on the elastic and thermal properties of the given material and the nature of the applied temperature distribution, are evaluated only once for each region. Once the $r_i$ coefficients are computed, the displacement particular integrals, $u_i^p$, are given by relations (30.1) and (30.2), and the traction particular integrals, $t_i^p$, by the following combinations of stresses assumed initially in relations (19.1)–(19.3):

$$t_1^p = \sigma_{11}^p n_1 + \sigma_{12}^p n_2 \tag{39.1}$$

$$t_2^p = \sigma_{12}^p n_1 + \sigma_{22}^p n_2 \tag{39.2}$$

where $n_1$ and $n_2$ are Cartesian components of the unit boundary normal.

The systematic procedure outlined above by relations (19.1) through (39.2) can easily be extended to the derivation of three-dimensional particular integrals and will not be

repeated here. We indicate below only the assumed temperature distribution $T(x_1, x_2, x_3)$ and the forms of stress-particular integrals $\sigma_{ij}^{p}$:

$$T(x_1, x_2, x_3) = t_0 + t_1 x_1 + t_2 x_2 + t_3 x_3 + t_{11} x_1^2 + t_{22} x_2^2 + t_{33} x_3^2 + t_{23} x_2 x_3 + t_{13} x_1 x_3 + t_{12} x_1 x_2 \quad (40)$$

$$\sigma_{11}^{p} = r_1 x_1 + r_2 x_1^2 + r_3 x_1 x_3 + r_4 x_1 x_2 \quad (41.1)$$

$$\sigma_{22}^{p} = r_5 x_2 + r_6 x_2^2 + r_7 x_2 x_3 + r_8 x_1 x_2 \quad (41.2)$$

$$\sigma_{33}^{p} = r_9 x_3 + r_{10} x_3^2 + r_{11} x_2 x_3 + r_{12} x_1 x_3 \quad (41.3)$$

$$\sigma_{23}^{p} = r_{13} x_2 + r_{14} x_3 + r_{15} x_2^2 + r_{16} x_3^2 + r_{17} x_2 x_3 + r_{18} x_1 x_3 + r_{19} x_1 x_2 \quad (41.4)$$

$$\sigma_{13}^{p} = r_{20} x_1 + r_{21} x_3 + r_{22} x_1^2 + r_{23} x_3^2 + r_{24} x_2 x_3 + r_{25} x_1 x_3 + r_{26} x_1 x_2 \quad (41.5)$$

$$\sigma_{12}^{p} = r_{27} x_1 + r_{28} x_2 + r_{29} x_1^2 + r_{30} x_2^2 + r_{31} x_2 x_3 + r_{32} x_1 x_3 + r_{33} x_1 x_2. \quad (41.6)$$

## NUMERICAL EXAMPLES

*Constrained composite plate under discontinuous temperature field*

Two plates of dimensions $l \times d$ are bonded together by a weld of thickness $p$, as shown in Fig. 1. Region (2) is raised to a temperature $T_0$ while regions (1) and (3) are held constant at the initial temperature. Under a condition of plane stress, the reduced compliance coefficients $B_{11}$, $B_{12}$, $B_{22}$ and $B_{66}$ are used for regions (1) and (3), and $b_{11}$, $b_{12}$, $b_{22}$ and $b_{66}$ are used for region (2). Furthermore, let the reduced thermal coefficients of linear expansion of region (2) be denoted as $\alpha_{11}$, $\alpha_{22}$ and $\alpha_{12}$. If all edges of the plate AFGD are supported on rollers to restrain movement in a direction normal to each edge, it may be shown that the following elastic solutions hold (assuming the origin of the coordinate system to be at A, with axis $x_1$ parallel to side AF):

$0 \leqslant x_1 \leqslant 2l + p$:

$$\sigma_{11} = \frac{\left(\frac{b_{12}}{b_{22}}\alpha_{22} - \alpha_{11}\right) p T_0}{2l\left(B_{11} - \frac{B_{12}^2}{B_{22}}\right) + p\left(b_{11} - \frac{b_{12}^2}{b_{22}}\right)} \quad (42.1)$$

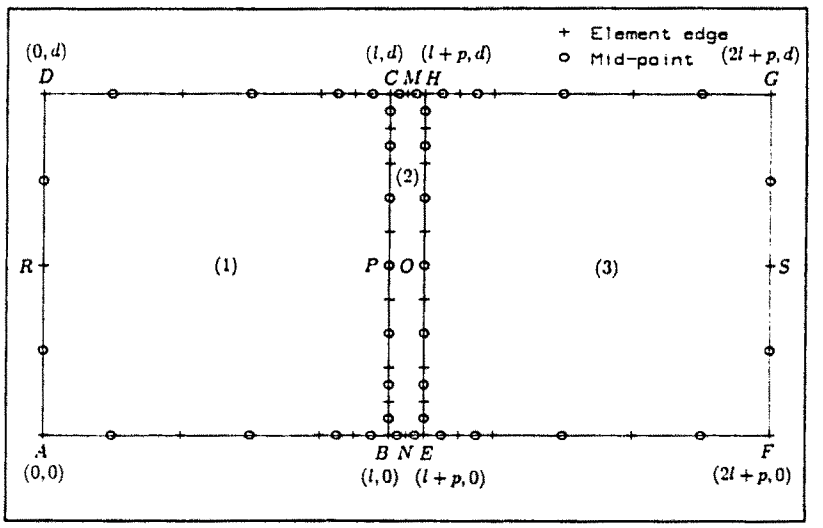


Fig. 1. Three-region boundary element model of composite plate.

$0 \leqslant x_1 < l,\ l+p < x_1 \leqslant 2l+p$:

$$\sigma_{22} = -\frac{B_{12}}{B_{22}}\sigma_{11} \tag{42.2}$$

$l < x_1 < l+p$:

$$\sigma_{22} = -\frac{1}{b_{22}}(b_{12}\sigma_{11}+\alpha_{22}T_0) \tag{42.3}$$

$0 \leqslant x_1 \leqslant 2l+p,\ 0 \leqslant x_2 \leqslant d$:

$$\sigma_{12} = 0 \tag{42.4}$$

$0 \leqslant x_1 \leqslant l$:

$$u_1 = \left(B_{11} - \frac{B_{12}^2}{B_{22}}\right)\sigma_{11}x_1 \tag{42.5}$$

$l \leqslant x_1 \leqslant l+p$:

$$u_1 = \left[\left(b_{11} - \frac{b_{12}^2}{b_{22}}\right)\sigma_{11} + \left(\alpha_{11} - \frac{b_{12}}{b_{22}}\alpha_{22}\right)T_0\right](x_1 - l) + \left(B_{11} - \frac{B_{12}^2}{B_{22}}\right)l\sigma_{11} \tag{42.6}$$

$l+p \leqslant x_1 \leqslant 2l+p$:

$$u_1 = \left(B_{11} - \frac{B_{12}^2}{B_{22}}\right)\sigma_{11}(x_1 - 2l - p) \tag{42.7}$$

$0 \leqslant x_1 \leqslant 2l+p,\ 0 \leqslant x_2 \leqslant d$:

$$u_2 = 0. \tag{42.8}$$

This problem was solved using the particular integral-based boundary element formulation. The following data were used:

$$B_{11} = 0.763, \quad B_{22} = 7.692, \quad B_{12} = -0.290 \tag{43.1}$$

$$b_{11} = 1.6, \quad b_{22} = 1.3, \quad b_{12} = -0.5 \tag{43.2}$$

$$\alpha_{11} = 0.001, \quad \alpha_{22} = 0.0015, \quad \alpha_{12} = 0.0 \tag{43.3}$$

$$l = 50, \quad p = 5, \quad d = 50 \tag{43.4}$$

$$T_0 = 100. \tag{43.5}$$

A three-region boundary element mesh employing three-noded quadratic elements is shown in Fig. 1. As shown in Table 3, the results obtained from the boundary element analysis are in excellent agreement with the analytical solutions given by relations (42.1)–(42.8).

Table 3. Comparison of BEM results with analytical solutions for a composite plate

| Point | | $\sigma_{11}$ | | $\sigma_{22}$ | | $u_1$ | |
|---|---|---|---|---|---|---|---|
| $x_1$ | $x_2$ | BEM | Analytical | BEM | Analytical | BEM | Analytical |
| 25. | 25 | −0.0096 | −0.0096 | −0.00036 | −0.00036 | −0.1804 | −0.1802 |
| 52.5 | 25 | −0.0096 | −0.0096 | −0.1192 | −0.1191 | 0.0000 | 0 |
| 80 | 25 | −0.0096 | −0.0096 | −0.00036 | −0.00036 | 0.1804 | 0.1802 |

*Freely expanding composite plate under discontinuous temperature field*

From the plate considered in the previous example, the geometric constraints are removed to allow it to deform freely, and the particular integral-based boundary element analysis is carried out. Rigid body movements are prevented by fixing point R (Fig. 1) in both the $x_1$- and $x_2$- directions, and fixing point S (Fig. 1) in the $x_2$-direction only. The deformed shape of the plate analyzed using the boundary element mesh in Fig. 1 is shown in Fig. 2. As the weld expands, regions (1) and (3) are subject to compression in the $x_1$-direction and mild tension in the $x_2$-direction, while region (2) is subject to compression in both the $x_1$- and $x_2$-directions. The variation of stresses $\sigma_{11}$ and $\sigma_{22}$ along the mid-section parallel to the $x_1$-direction is shown in Fig. 3. [Point P represents the position of the interface between regions (1) and (3).] Stresses are plotted for one half of the plate (from R to O in Fig. 1). The dominant stress $\sigma_{22}$ is shown in Fig. 4 through the mid-section MN parallel to the $x_2$-direction. The effect of changing the specially orthotropic properties to general orthotropy has also been studied. In the material property data in (43.1)–(43.3), the major principal axis is assumed to be parallel to the $x_1$-direction ($\theta = 0^\circ$). The major principal axes in regions (1) and (3) are gradually rotated counterclockwise to a position 90° to the $x_1$-direction ($\theta = 90^\circ$). The variations of stresses with respect to the orientation of the principal material direction at an interfacial point P are shown in Fig. 5. As expected, there is a relaxation of $\sigma_{11}$ at P because of weakening of regions (1) and (3) in the $x_1$-direction, and a simultaneous build-up of $\sigma_{22}$ both to the left and the right of P. The shear stress $\sigma_{12}$ (Fig. 5) vanishes in the initial and final specially orthotropic positions, and reaches a maximum value in between these positions.

*Multi-layer cantilever under linear temperature distribution*

A three-layer anisotropic cantilever is analyzed for a linear temperature distribution through the thickness by the two-dimensional (plane stress) particular integral-based boundary element formulation. Each orthotropic layer is modeled as a substructured region in the boundary element analysis. A typical boundary element mesh with 24 quadratic elements per region is shown in Fig. 6. Regions ABQP and RSCD are assigned elastic properties identical to those in regions (1) and (3) in the first example. In addition, the following coefficients of linear thermal expansion are assumed:

$$\alpha_{11} = 0.001, \quad \alpha_{22} = 0.002, \quad \alpha_{12} = 0.0. \tag{44.1}$$

The elastic and thermal properties of the region PQSR are identical to those of the

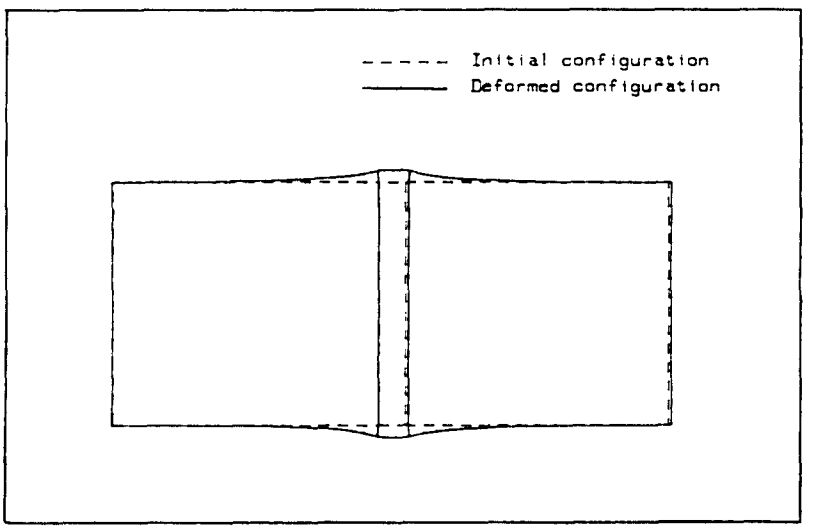


Fig. 2. Thermally loaded composite plate undergoing free expansion.

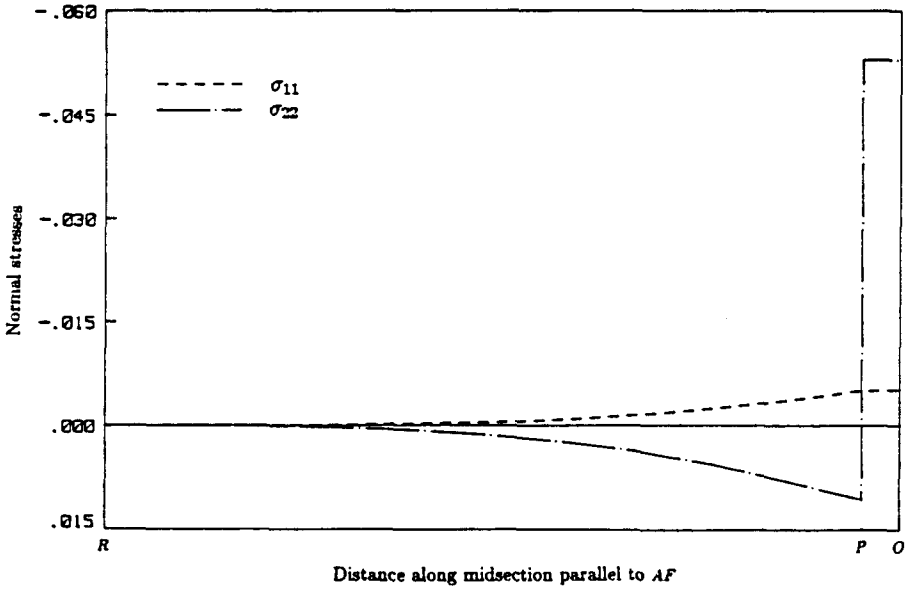


Fig. 3. Variations of $\sigma_{11}$ and $\sigma_{22}$ along the mid-section R–P–O.

weld [region (2)] in the first example. With the $x_1$- and $x_2$-axes oriented along the sides AB and AD, respectively (Fig. 6), the following temperature distribution is assigned:

$$T = 0.01x_2. \tag{44.2}$$

In general, it is also assumed that the major principal axes in the bottom and top layers ABQP and RSCD are oriented at $0^\circ$-clockwise and $0^\circ$-counterclockwise respectively with respect to the $x_1$-direction; the middle layer is, however, specially orthotropic with the major principal axis aligned parallel to the $x_1$-axis.

In Fig. 7, the results of the convergence study of the free-end deflection with respect to the number of elements per region are presented for three different cases of fiber

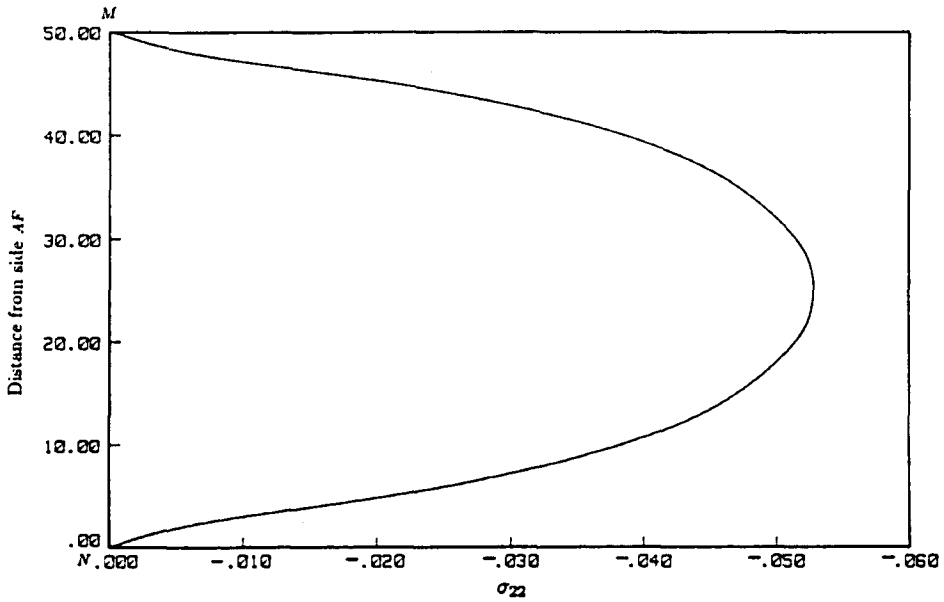


Fig. 4. Variation of $\sigma_{22}$ along the mid-section MN.

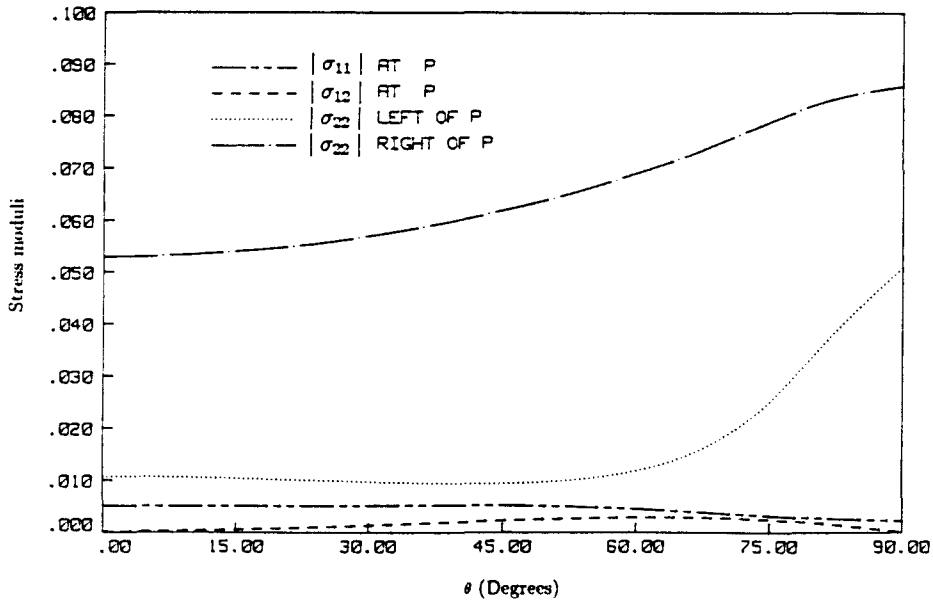


Fig. 5. Variations of absolute values of stresses with fiber orientation.

orientation ($\theta = 0^\circ$, $45^\circ$ and $90^\circ$) and distinct patterns of convergence are observed. The effect of fiber orientation on the free-end deflection (i.e. overall beam stiffness) is shown in Fig. 8, where a rather abrupt loosening of the cantilever stiffness is noticed for an orientation roughly given by $\theta = 45^\circ$. In Fig. 9 (where the dotted lines represent the inter-layer boundaries), mid-span through-the-depth bending stresses are presented for $\theta = 45^\circ$ and $90^\circ$. The bending stresses for $\theta = 0^\circ$ are negligible as compared to those for $\theta = 45^\circ$ and $90^\circ$ and hence are not shown. It is of interest to note that bending stresses vary in a piecewise linear fashion through the depth as would normally be predicted by a laminate-beam theory.

*Comparison between an anisotropic cube and a square plate using particular integrals*

Because of the rather extensive algebra involved in developing the expressions of the three-dimensional particular integrals, it is essential to carefully check the correctness of these integrals. A simple way of doing so is to develop test cases for comparing plane strain

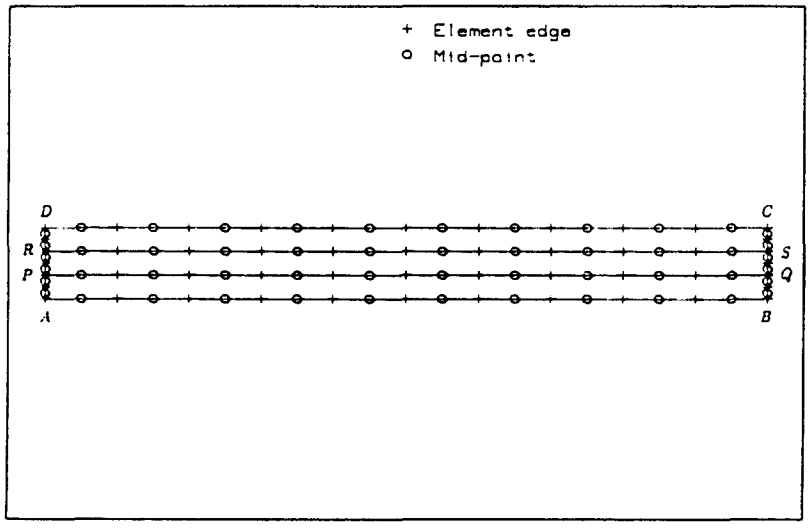


Fig. 6. Boundary element model of three-layer cantilever.

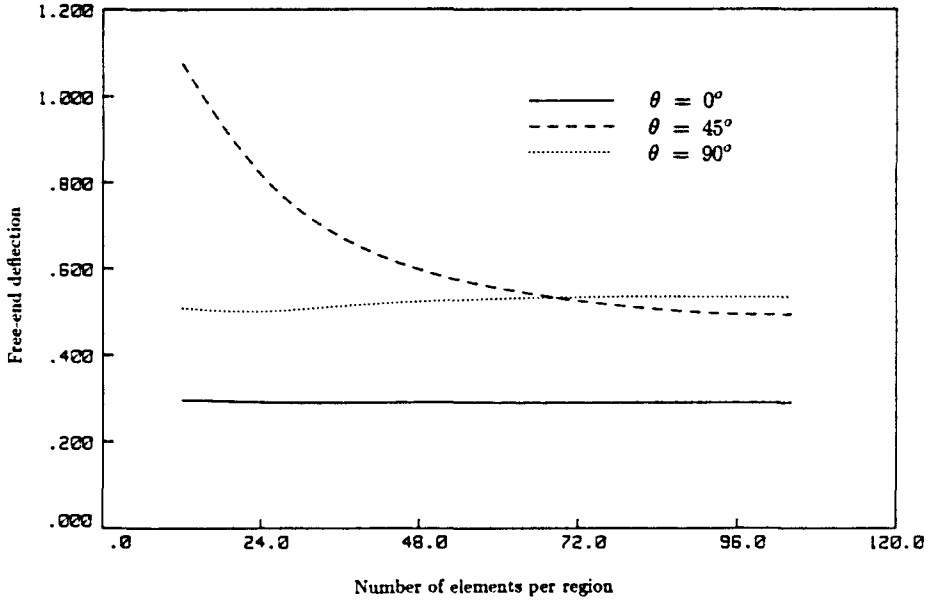


Fig. 7. Convergence studies of deflection.

analysis with the corresponding three-dimensional analysis where plane strain behavior is enforced by restricting any movement in the $x_1$-, $x_2$- or $x_3$-directions. As an exmple, the following material data are assumed pertaining to a fictitious monoclinic material with 13 independent elastic constants:

$$b_{11} = 1.6, \quad b_{12} = -0.5, \quad b_{13} = -0.3, \quad b_{16} = 0.1 \tag{45.1}$$

$$b_{22} = 1.3, \quad b_{23} = -0.4, \quad b_{26} = 0.13 \tag{45.2}$$

$$b_{33} = 1.0, \quad b_{36} = 0.16 \tag{45.3}$$

$$b_{44} = 1.0, \quad b_{45} = 0. \tag{45.4}$$

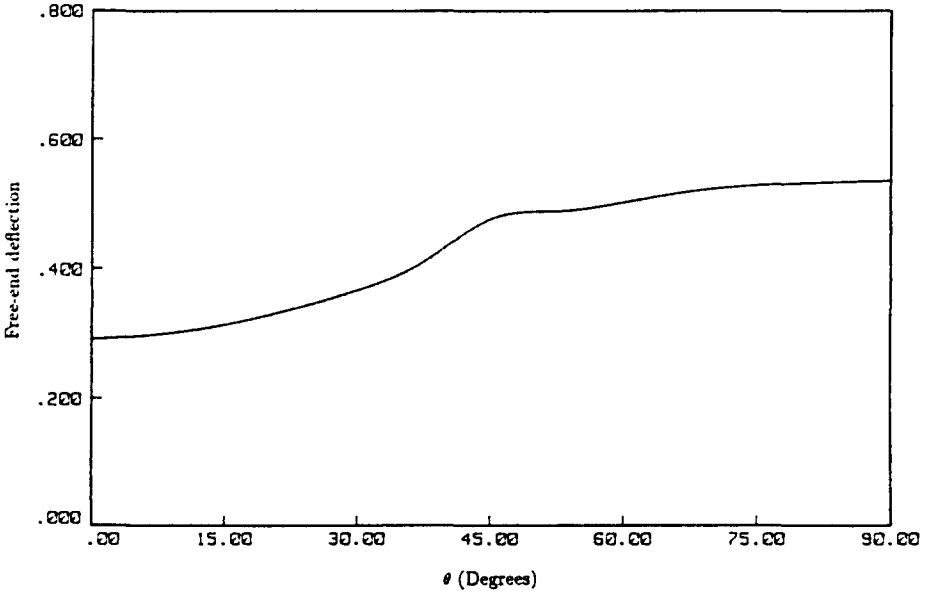


Fig. 8. Variation of deflection with fiber orientation.

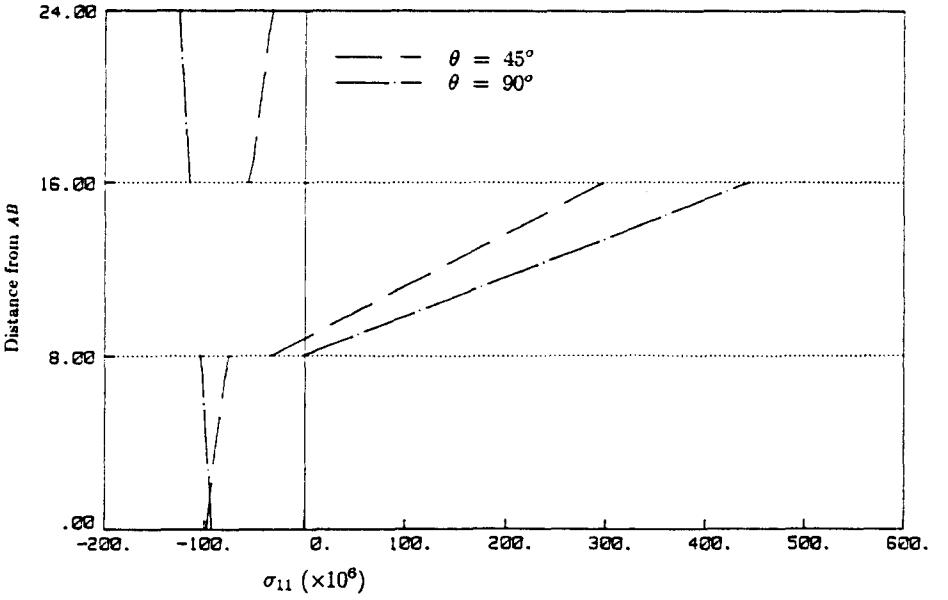


Fig. 9. Mid-span bending stresses through cantilever depth.

$$b_{55} = 1.0 \tag{45.5}$$

$$b_{66} = 2.8. \tag{45.6}$$

The angle of inclination of the major material axis with the $x_1$-direction = 30 ;

$$\alpha_{11} = \alpha_{22} = \alpha_{33} = 0.001, \quad \alpha_{23} = \alpha_{13} = \alpha_{12} = 0.0. \tag{45.7), (45.8}$$

The material described above is respectively in the form of a unit square plate and a unit cube for two- and three-dimensional analysis.

The following temperature distribution is now assumed:

$$T = 1 + x_1. \tag{45.9}$$

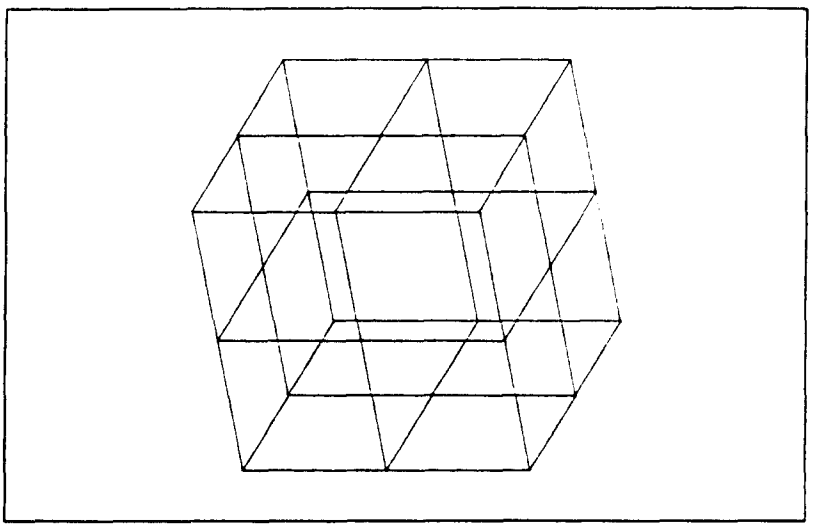

Fig. 10. Unit cube with four quadrilateral elements per face.

Table 4. Comparison of 2D and 3D analyses using particular integrals

| Displacement | BEM (2D) | BEM (3D) |
|---|---|---|
| $u_1$ | $0.8713 \times 10^{-3}$ | $0.8715 \times 10^{-3}$ |
| $u_2$ | $0.2079 \times 10^{-4}$ | $0.2094 \times 10^{-4}$ |

Table 5. Comparison of 2D and 3D analyses using volume integration

| Displacement | BEM (2D) | BEM (3D) |
|---|---|---|
| $u_1$ | $0.6982 \times 10^{-3}$ | $0.6977 \times 10^{-3}$ |
| $u_2$ | $0.6488 \times 10^{-3}$ | $0.6490 \times 10^{-3}$ |

The two-dimensional boundary element mesh consists of two quadratic elements per side of the unit square plate. For three-dimensional analysis, the boundary element model consisting of four quadratic elements per face of the unit cube is used, as shown in Fig. 10. Displacements are compared at the center (0.5, 0.5) of the square plate with those at the center (0.5, 0.5, 0.5) of the cube in Table 4 and excellent agreement is observed.

*Comparison between an anisotropic cube and a square plate by volume integration*

The unit square plate and the cube described in the previous example are subject to a uniform temperature [i.e. $x_1 = 0$ in eqn (45.9)] of unity and solved by volume integration by considering one eight-noded planar cell (with one three-noded quadratic element per side) and one 20-noded three-dimensional cell (with one eight-noded quadrilateral element per face). The results (at the centers of the plate and the cube) of the two- and three-dimensional analyses match extremely well, as apparent from Table 5.

## CONCLUSIONS

New boundary element formulations are introduced for the elastic analysis of two- and three-dimensional anisotropic bodies subjected to thermal body forces. The body force point-of-view of the temperature gradients is adopted, and volume integration and particular integral-based approaches are described. Effective particular integrals are presented for a quadratic temperature distribution on plane as well as in three dimensions. A systematic procedure, extremely useful in the derivation of the arbitrary particular integrals, has been outlined. For an arbitrary temperature distribution in a sub-domain, either the method of volume integration or the more efficient particular integral-based approach may be followed; in the latter case, by fitting a quadratic polynomial to the given temperature distribution via a multi-regression analysis. The formulations presented have been implemented in a general purpose multi-region boundary element code, namely GPBEST, and validated with examples.

*Acknowledgements*—The authors would like to thank Professor P. K. Banerjee for his valuable advice and encouragement. Funding for this work was proved by Pratt and Whitney Aircraft, Hartford, Connecticut.

## REFERENCES

Banerjee, P. K. and Butterfield, R. (1981). *Boundary Element Methods in Engineering Science*. McGraw-Hill, London.

Banerjee, P. K., Henry, D. P., Jr. and Raveendra, S. T. (1989) Advanced inelastic analysis of solids by the boundary element method. *Int. J. Mech. Sci.* **31**, 309–322.

Banerjee, P. K. and Raveendra, S. T. (1986). Advanced boundary element analysis of two- and three-dimensional problems of elastoplasticity. *Int. J. Numer. Meth. Engng* **23**, 985–1002.

Cruse, T. A. (1973). Application of the boundary integral equation method to three-dimensional stress analysis. *Comput. Struct.* **3**, 509–527.

Cruse, T. A. (1974). An improved boundary integral equation method for three-dimensional stress analysis. *Comput. Struct.* **4**, 741–757.

Henry (Jr), D. P. and Banerjee, P. K. (1988). A new boundary element formulation for two- and three-dimensional thermoelasticity using particular integrals. *Int. J. Numer. Meth. Engng* **26**, 2061–2077.

Jaswon, M. A. and Maiti, M. (1968). An integral equation formulation of plate bending problems. *J. Engng Math.* **2**, 83–93.

Lachat, J. C. and Watson, J. O. (1976). Effective numerical treatment of boundary integral equations: a formulation for three-dimensional elastostatics. *Int. J. Numer. Meth. Engng* **10**, 991–1005.

Lekhnitskii, S. G. (1968). *Anisotopic Plates*. Gordon and Breach, New York.

Malen, K. (1971). A unified six-dimensional treatment of elastic Green's functions and dislocations. *Phys. Stat. Sol.* **44**(6), 661–672.

Nowacki, W. (1986). *Thermoelasticity*, 2 Edn. PWN—Polish Scientific Publishers, Warsaw.

Padovan, J. (1986). Anisotropic thermal stress analysis. In *Thermal Streesses* I (Edited by R. B. Metnarski), pp. 143–262. Elsevier, Amsterdam.

Pape, D. A. and Banerjee, P. K. (1987). Treatment of body forces in 2D elastostatic BEM using particular integrals. *J. Appl. Mech.* **54**, 866–871.

Rizzo, F. J. and Shippy, D. J. (1968). A formulation and solution procedure for the general non-homogeneous elastic inclusion problem. *Int. J. Solids Structures* **4**, 1161–1179.

Rizzo, F. J. and Shippy, D. J. (1977). An advanced boundary integral equation method for three-dimensional thermoelasticity. *Int. J. Num. Meth. Engng* **11**, 1753–1768.

Snyder, M. D. and Cruse, T. A. (1975). Boundary-integral equation analysis of cracked anisotropic plates. *Int. J. Fracture* **11**, 315–328.

Synge, J. L. (1957). *The Hypercircle in Mathematical Physics*, pp. 411–413. Cambridge University Press, U.K.

Vogel, S. M. and Rizzo, F. J. (1973). An integral equation formulation of three-dimensional anisotropic elastostatic boundary value problems. *J. Elasticity* **3**, 203–216.

Watson, J. O. (1979). Advanced implementation of the boundary element method for two- and three-dimensional elastostatics. In *Developments in Boundary Element Methods*—1. (Edited by P. K. Banerjee and R. Butterfield), pp. 31–63. Applied Science, London.

Wilson, R. B. and Cruse, T. A. (1978). Efficient implementation of anisotropic three-dimensional boundary integral equation stress analysis. *Int. J. Numer. Meth. Engng* **12**, 1383–1397.